JOURNAL OF MECHANICS OF CONTINUA AND MATHEMATICAL SCIENCES
www.journalimcms.org

ISSN (Online) : 2454 -7190 , Special Issue, No.-11, May (2024) pp 186-199 ISSN (Print) 0973-8975

DERMONET: LIGHTWEIGHT DIAGNOSTIC SYSTEM FOR DERMATOLOGICAL CONDITIONS USING SQUEEZENET FRAMEWORK

Poonam Dhiman[1], Shivani Wadhwa[2], Aryan Choudhary[3] Amandeep Kaur[4], Khushpreet Malra[5]

[1]Government PG College, Ambala Cantt 133001, India.

[2,4,5] Chitkara University Institute of Engineering and Technology, Chitkara University, Punjab, India.

[3]Software Engineer, Nurdsoft.co, Los Angeles, USA.

Email : [1]drpoonamdhiman19@gmail.com , [2]shivani.wadhwa@chitkara.edu.in, [3]sep2001aryan@yahoo.com, [4]amandeep@chitkara.edu.in, [5]khushpreet1988.be21@chitkara.edu.in

Corresponding Author: **Poonam Dhiman**

https://doi.org/10.26782/jmcms.spl.11/2024.05.00013

(Received: March 14, 2024; Revised: April 28, 2024; Accepted: May 17, 2024)

Abstract

Skin malignancies are regarded as the most dangerous disease. Skin cancer has recently received much attention among people worldwide. An earlier diagnosis of skin cancer can lower the mortality rate. Skin cancer can be found and identified via dermoscopy. Automated tools using computer-aided diagnosis models become necessary because visually evaluating dermoscopic images is tedious and time-consuming. The healthcare industry has greatly benefited from recent machine learning advancements like deep learning. Modern technical designs and methodologies make detecting this type of cancer possible; however, automated classification in earlier phases is challenging due to the lack of contrast. As a result, a squeeze net algorithm-based automated computer system is developed for diagnosing skin illnesses. The HAM10000 dataset is gathered for skin lesions. Images of the four skin cancer conditions BCC, DF, MEL, BKL, and NV are included in the dataset. With a 92.25% overall accuracy, 85% precision, 84% recall, and 83% F1 score, the proposed dermonet model did well in classifying skin cancer conditions from the image samples.

Keywords: skin lesions, squeeze net, classification, feature extraction, deep learning.

I. Introduction

Machine learning is geared to be a powerful tool for advancing medical diagnostics, particularly when combined with highly intricate neural networks and robust hardware. Nonetheless, the cost of such gear and the need for persistent internet

connectivity pose obstacles, especially in areas where reliable access to the internet is restricted [IX]. Skin cancer, particularly melanoma, is a major hazard in neglected areas such as impoverished rural communities and developing countries. Unfortunately, early signs of skin cancer are not always discernible, leading to diagnostic outcomes heavily reliant on the expertise of dermatologists. For less experienced practitioners, an automated diagnostic system emerges as a vital tool to enhance accuracy in diagnosis [XVI]. The necessity for performance improvement in the ImageNet challenge led to the creation of AlexNet. It was one of the first times deep convolutional networks had achieved such excellent accuracy. The SqueezeNet model consequently diverted from the norm to become more compact. The network simplified its structure to increase efficiency by switching out 3x3 kernels for 1x1 kernels. This change resulted from the fact that 1x1 kernels require just 9 times as few parameters as their 3x3 equivalents. This modification was justified by reducing network parameters without sacrificing performance. Notably, SqueezeNet achieved the contest for pruning due to its fully convolutional structure and modern architectural architecture [V].

I.i Contribution of Paper

This study has built a new computer-aided diagnostic model for effectively identifying and classifying skin cancer using dermoscopic pictures driven by an ideal deep neural network. This study applies deep learning advancements to medical imaging. The first step is pre-processing an image by gathering it from a database and then rescaling, normalizing, and augmenting data. The entire collection of skin lesion image samples is collected from the well-known HAM10000 database to train our models. SqueezeNet is a compact CNN architecture that is presented. The proposed model is also contrasted with other cutting-edge methods. Smaller suggested CNN architectures need less bandwidth and communication between servers during distributed training to achieve a similar level of accuracy. The suggested model is easier to implement on systems with little memory.

I.ii. Organization of Paper

This paper's structure is divided into six sections, which are as follows: With a focus on its utility in skin lesion identification, the first section offers a thorough assessment. A full review of the body of existing research is provided in the second section. The third section lists the materials and methods employed in this research. A detailed explanation of the modifications made to existing models, as well as the technique utilized to build our models, are provided in the fourth section. Results from the experiments are discussed in the fifth section. The paper's conclusion is presented in the final part.

II. Literature Review

The difficulty of accurately separating skin anomalies from skin cancer lesions is growing as the number of instances of skin cancer each year rises, especially the dangerous type known as malignant melanoma. Factors like artifacts, low contrast, and visual resemblances to benign structures like moles or scars complicate this.

[IV] emphasizes accuracy and efficiency while using cutting-edge techniques for automated skin lesion diagnosis. It improves early diagnosis by utilizing robust feature extraction using the ABCD rule, GLCM, and HOG. Geodesic Active Contour (GAC) effectively isolates lesion regions while pre-processing enhances picture quality. Metrics for symmetry, boundaries, colour, and texture are among the features. SVM, KNN, and Naive Bayes classifiers distinguish between benign and malignant lesions for machine learning. Impressive performance is shown during testing on an ISIC dataset with 97.8% accuracy, SVM AUC of 0.94, and KNN at 86.2% sensitivity and 85% specificity.

Skin cancer [XIV] is a dangerous and potentially fatal condition, and chances of survival are greatly increased by early identification. Early detection is difficult and expensive since malignant growths closely mimic benign moles. The discomfort and scarring associated with surgical evaluation highlight the need for a non-invasive, precise detection method.

The traditional Support Vector Machine (SVM) and Deep Learning (DL) models ResNetv2, EfficientNet-B7, EfficientNet-B5, and VGG16 are contrasted in [XI] work to diagnose skin cancer automatically. The outcomes favour the CNN models, especially EfficientNet-B7, which achieves an outstanding F1 score of 84.22%. This highlights the promise of cutting-edge DL techniques for skin cancer diagnosis [XVIII]. The Python-based CNN classification model uses Keras and Tensorflow as the backend. The model is constructed by altering the types of layers used to train the network and evaluated using various network topologies. For early convergence, the model also applies transfer learning approaches[VII].

CNNs are receiving much attention in the area of automated melanoma detection, a serious type of skin cancer [XII]. This work provides a unique approach to early skin cancer identification using dermoscopic pictures. Our model is based on the well-known VGG-16 architecture, but we have improved it to increase its efficacy in detecting skin cancer. We used the International Skin Image Collaboration dataset to compare our method and previously recognized approaches to evaluate our approach. The outcomes show that our model outperforms other methods in accuracy [III].

To detect and categorize skin cancer, this research offers a decision support system that uses convolutional neural networks (CNN). The CNN-based approach promises to improve accuracy and efficiency by offering helpful insights and aid in detecting skin cancer [VI] describes a method for categorizing skin cancer using convolutional neural networks (CNN). It includes information on the CNN architecture, data pretreatment methods, and test results. The study shows that CNNs can classify skin lesions accurately, showing promise for automated skin cancer diagnosis.

III. Material and Methods

Data gathering, model training, and multi-class classification of skin lesion images are some processes in developing a framework for detecting and classifying skin diseases [XV]. The general organization of this proposed framework is depicted in Fig. 1 using a block diagram. It represents major steps followed by the proposed framework using the squeeze net model for skin disease detection and classification.

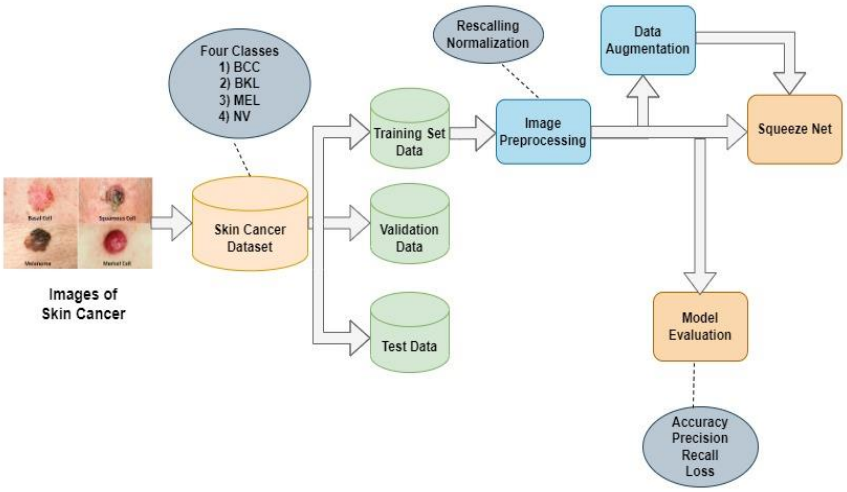

Fig. 1. Block Diagram for Detection and Classification of Skin Disease

III.i. Dataset Used

Fig. 2 represents a few samples of skin lesions. 10,000 training image samples from a dataset called HAM10000 [XIII] provide a distinctive human-versus-machine collection. The newest public library of skin lesions, this dataset tackles a long-standing issue with diversity constraints. The result of diligent work, the HAM10000 dataset, includes 10,015 dermoscopic images from two different sources: the dermatology department of the Medical University of Vienna in Austria and Cliff Rosendahl's skin cancer clinic in Queensland, Australia. This vast collection was assembled over twenty years. Physical image printouts of lesions were kept at the Dermatology Department of the Medical University of Vienna, Austria, before the advent of widely used digital images.

The images were subjected to various acquisition functions and cleansing processes to improve the dataset's quality and diversity. A semi-automatic approach driven by a neural network was developed to inject variation into the dataset further. The dataset includes images of 514 basal cell carcinomas, 1099 benign keratoses, 1113 melanocytic nevi, and 6705 melanomas. Table 1 represents the description of common skin disease types.

Table 1: Description of Skin Diseases

Skin Disease Type	Description	Reference
Actinic keratoses and intraepithelial carcinoma / Bowen's disease (AKIEC)	The most common neoplastic skin lesion, actinic keratosis, is an intraepidermal squamous tumour of sun-damaged skin.	[IV], [XI]
Basal cell carcinoma	The most prevalent variant of skin cancer is basal-cell carcinoma (BCC), often known as basal-cell cancer. It typically presents as a painless raised area on the skin, which may have a glossy appearance and exhibit tiny blood vessels. Alternatively, it can manifest as a raised area with an ulcer. Basal-cell carcinoma typically exhibits slow growth and can potentially affect adjacent	[XVIII]

	tissue, although it is rarely prone to metastasis or considered life-threatening.	
Benign keratosis-like lesions	Common benign skin lesions include lichen planus-like keratosis seborrheic keratosis, and solar lentigo. These lesions can develop from one another or are frequently found next to one another. Despite possessing distinct histological characteristics, they can occasionally be difficult to distinguish.	[VII]
Dermatofibroma (DF)	It is a common kind of cutaneous lesion. Women are more likely to experience this illness than men. Dermatofibroma typically develops on the extremities, especially the lower legs, and frequently has no symptoms. Although it is mostly asymptomatic, discomfort and pruritus (itchiness) can occasionally appear.	[XII]
Melanoma	It is a type of cancer of the skin, that begins in Melanocytes, the cells responsible for controlling skin pigmentation. In the depicted diagram, you can observe melanoma cells infiltrating the deeper layers of the skin beyond its surface.	[III]
Congenital melanocytic nevus (CMN)	A skin defect known as a congenital melanocytic nevus is defined by the benign proliferation of nevomelanocytes, which are cells that produce pigment. These nevi appear at birth or within the first several weeks after birth. They are sometimes called "giant hairy nevi" since they frequently have excessive hair growth growing alongside them.	[VI]
Vascular lesions	Vascular lesions, frequently called birthmarks, are common irregularities affecting the skin and the underlying tissues. These vascular lesions are typically categorized into three primary groups: hemangiomas, vascular malformations, and pyogenic granulomas.	[XV]

III.ii. Data Augmentation

Enhancements were made for each image in the collection by creating augmented versions and related masks. These additions included controlled zooming, width and height modifications, rotations within a certain range, and horizontal flips [XXI]. A smart approach was used to address the uneven distribution of classes across skin cancer categories: oversampling the picture samples from underrepresented classes made possible using randomized augmentation techniques. On the HAM10000 dataset, a deliberate separation was implemented to guarantee impartial predictions and prevent skewed results. The training set, validation set, and evaluation set are three separate sets that this division produced. Aiming to reduce the risk of overfitting, such a technique ensured that the models' performance would translate well to new data [XIX]. Fig.2. represents the sample collected for different skin diseases.

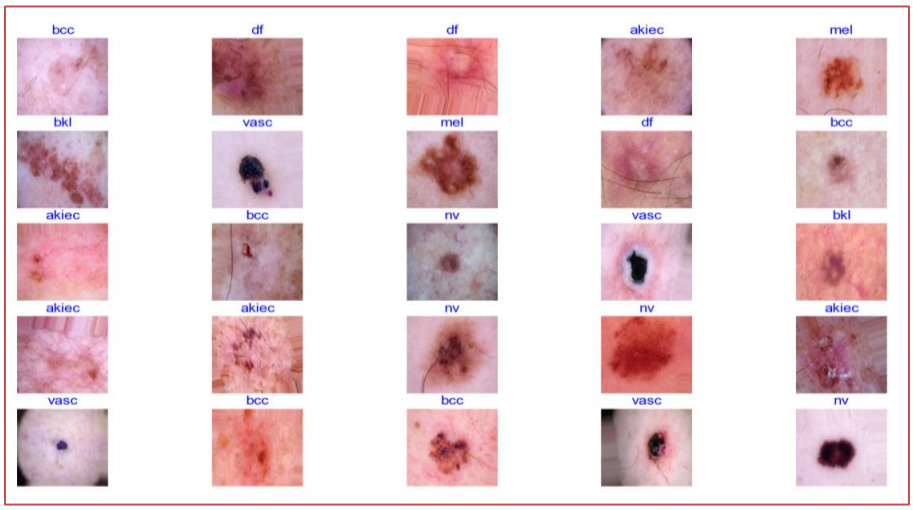

Fig. 2. Skin Lesion Samples

III.iii. SqueezeNet

SqueezeNet, a compact CNN architecture, is described, which astonishingly meets AlexNet's accuracy test on the ImageNet dataset despite using far fewer parameters, 50 times fewer, to be precise. Several applications benefit from this streamlined architecture. It excels at effective distributed training and incurs little overhead when delivering new models to clients. Additionally, it works well in contexts with limited resources and is deployable on FPGA and embedded systems [XVII]. SqueezeNet's characteristic fire module is at its core, which serves as its essential building piece. Each fire module has a squeeze layer employing kernels of a (1, 1) size.

III.iii.a. DermoNet using SqueezeNet Architecture

A significant choice was made in favour of 1x1 filters in pursuing convolution filter optimization within a predetermined parameter budget. The main factor influencing this decision is the 1x1 filter's drastically decreased parameter count, which is only a ninth of a 3x3 filter's. The computing demand of a 1x1 filter requires fewer accumulators when implemented on a chip, resulting in a nine-fold reduction in computation time compared to its 3x3 counterpart. Imagine a convolutional layer with only 3x3 filters in it [X].

The formula for this layer's total parameter count is (number of input channels) x (number of filters) x (3x3). Convolution has one disadvantage, though the information loss along the edge of the image. Padding is cleverly used within the SqueezeNet framework to get around this, but only in the fire module. This procedure involves adding layers of zeros to the input image to ensure that the output feature map retains its dimensions despite accumulating convolutional layers [XXII]. A crucial technique routinely used for each input activation value is rectified linear activation (ReLU). Its

purpose is to maintain positive values while converting negative values in the feature map to zeros. This process follows Equation 1's computation.

$$g(i) = \begin{cases} 0, & i < 0 \\ i, & i \geq 0 \end{cases} \quad (1)$$

A key component influencing how CNNs function is the convolutional layer. Its parameters are set up to support the use of flexible kernels. These kernels often span the entire depth of the input data while having compact spatial dimensions. Each filter is convolved across the spatial dimensions of the input during the encounter with a convolutional layer, producing a 2D activation map. The task includes aggregating the contributions from the cells. Z_{xy}^{m} is of the previous layer to determine the input preceding nonlinearity for a specific unit Z_{xy}^{m} within the proposed model layer. The components of the respective filters are used to determine how much weight to give these contributions [VIII]. The task included in equation 2

$$Z_{xy}^{m} = \sum_{i=0}^{n-1} \sum_{j=0}^{n-1} \omega_{ij}\, q_{(x+i)(y+j)}^{m-1} \quad (2)$$

III.iii.b. Fire Module

A fire module comprises two convolutional layers integrated in succession, each followed by a ReLU layer. The first layer is known as the "squeeze layer," while the second is known as the "expand layer." The output picture dimension is 55 x 55 x 16, starting with an input image dimension of 55 x 55 x 96. The stride value is left at 1, and the filter size for the squeeze layer is set to 1x 1. With the same parameters as the input image, this strategic setup maintains the output image's width and height [II]. The squeeze convolutional layer's output is fed into the following expand layer. The convolutional layer representing the expand layer successfully incorporates 1×1 and 3×3 filters. This design operates within the constraints of dimensions. A comprehensive 128-channel output is produced due to the smooth interaction between the 64 output channels from the 1×1 convolutional filter and the 3×3 convolutional filter. Within the output image, the 1×1 convolution's output channels are located in the range of channels 1-64, whereas the 3×3 convolution's output channels occupy the positions of channels 65–128 [XXIV].

The maxpool and average pooling layers are two different categories used in SqueezeNet. Pooling layers serves the core goal of downsampling, an activity designed to reduce the complexity of succeeding layers. This idea has analogies to decreasing resolution without affecting channel count in image processing. The softmax layer, used as the top layer, accurately transforms the neural network output into a probability distribution covering K-predicted outcome categories. The following algorithm has been used for implementing the proposed technique. Fig. 3 presents the architecture of our squeeze Net model.

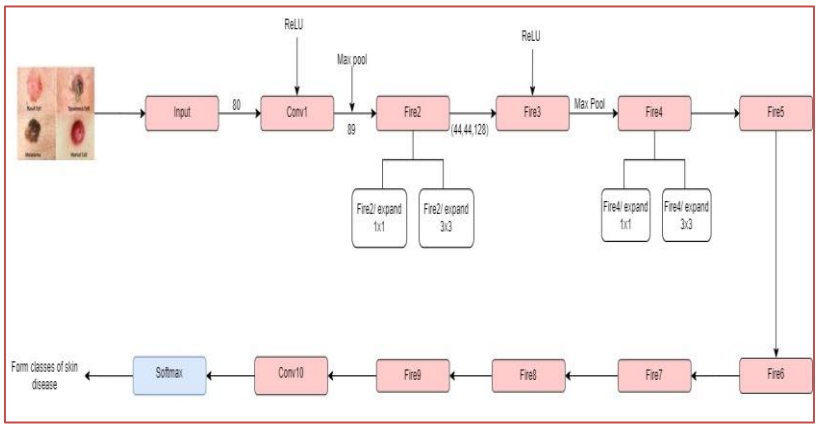

Fig. 3. Architecture of Squeeze Net

Proposed Algorithm 1

Let img = skin cancer image, aug = augmentation, pix_val=pixel value

Input: Read images of Skin Cancer from HAM10000}

Output: {confusion matrix, accuracy, loss, precision, f-score, recall}

Step 1: Input(img(n))

Step 2: Read CSV files

Step 3: Set the Threshold value for the img data generator

Step 4: perform img pre-processing

4.1. Resize (img)/224*24*3

4.2. Normalize pix_val (img)/interval [0,1]

Step 5: Perform data randomized aug(img)

5.1. horizontal flip (img)

5.2. rotation range(img,20)

5.3. width_shift_range(img,0.2)

5.4. height_shift_range(img,0.2)

5.5. zoom_range(img,0.2)

Step 6: Prepare (img samples)/training, testing, and validating

Step 7: Implement the Squeeze_net model

7.1. Create a fire module of the squeeze_net model

7.2. Create (fire2…n /relu_sequeeze 1× 1)

7.2.1. Create (fire 2…n/expand 1× 1)

7.2.2. Create (fire 2…n/expand 3× 3)

7.2.3. Create (fire 2…n/concat(pix_val))

7.3. global_avg_pooling(pix_val)

Step 8: Fine-tune parameters (fire module, layers, learning rate, epochs, batch size)

Step 9: Evaluate the Performance of the Model using different metrics

Step 10: Perform Evaluation (existing work)

IV. Training and Testing

Several tests using the HAM10000 dataset were collected to evaluate the effectiveness of the employed DL approach and make comparisons with the present state of the art. Additionally, simulations were run on the ISIC2018 dataset to evaluate how well the proposed DL systems performed compared to industry standards. A ratio of 80:20 was used to divide the dataset into training and testing sets. All subsequent testing was conducted using the training set created by randomly choosing 80% of the lesion images. Additionally, 10% of the data was set aside for validation during the learning phase.

The weight combinations that produced the best accuracy rates were kept. The suggested architecture was trained using the Adam optimizer on the HAM10000 dataset. To solve validation patience, this optimizer uses a learning rate approach intended to slow down learning when it shows stagnation for an extended period. A batch rebalancing method was implemented to further improve the representation of infection types in the batching process. Using a batch size of 32, this method helped to correct the overrepresentation of distinct classes within the batches. Fig. 4 represents the feature extracted from the skin lesion images using the squeeze net model.

5. Result and Discussion

In this study, four different kinds of skin cancer: basal cell carcinoma, benign keratosis-like lesions, dermatofibroma, melanoma, and melanocytic nevi are distinguished using a suggested classification based on the structure of a deep neural network. Utilizing traditional evaluation criteria, the effectiveness of the proposed strategy was determined. Measures in the above research included accuracy, the F1-score, recall, specificity, and precision. The suggested classification system's effectiveness was evaluated using the HAM10000 dataset using four statistical indices: false positive, true negative, false negative, and true positive.

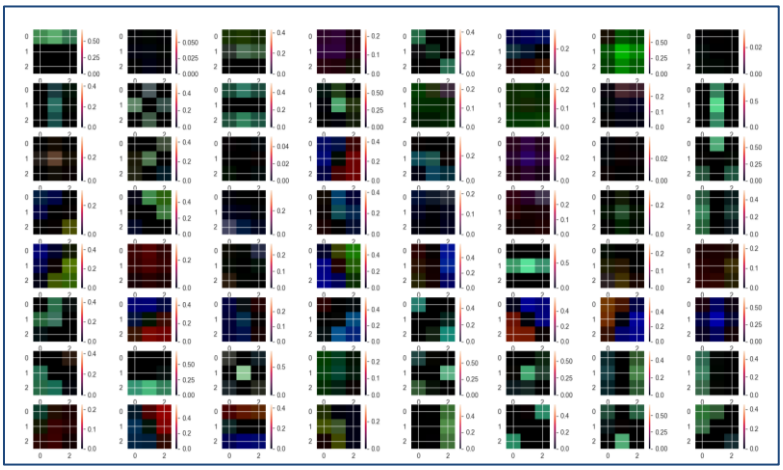

Fig.4. Feature Extracted from Squeeze Net

Confusion matrices are also employed to correctly evaluate data that contains predictions and ground truth labels in Table 2. The diagonal elements represent the true positives, which are inversely correlated with the trained model's total accuracy. Each fold of cross-validation has its confusion matrix. On the validation data set, it has been demonstrated that the suggested model has produced extremely accurate results. For bcc, bkl, mel, and nv, respectively, the trained model attained an accuracy of 93.25%, 90.5%, 93.75%, and 91.75%. On various folds, it has an average cross-validation accuracy of 92.93%. Table 3 displays each class's recall, precision, and F1 score. The average precision, recall, and F1-score values are 85%, 84%, and 83%, respectively. Fig. 5 represents the training and validation curve of loss, accuracy, and f1-score on epochs for the squeeze model.

Table 2. Confusion Matrix for Different Classes

Class	BCC	BKL	MEL	NV
BCC	87	8	7	5
BKL	6	79	4	11
MEL	4	9	83	8
NV	3	4	6	76

Table. 4. Performance Evaluation on Test Dataset

Class	Accuracy	Precision	Recall	F1Score
BCC	93.25	84	90	87
BKL	90.5	80	82	81
MEL	93.75	88	87	87
NV	91.75	86	79	82
Overall	92.93	85	84	83

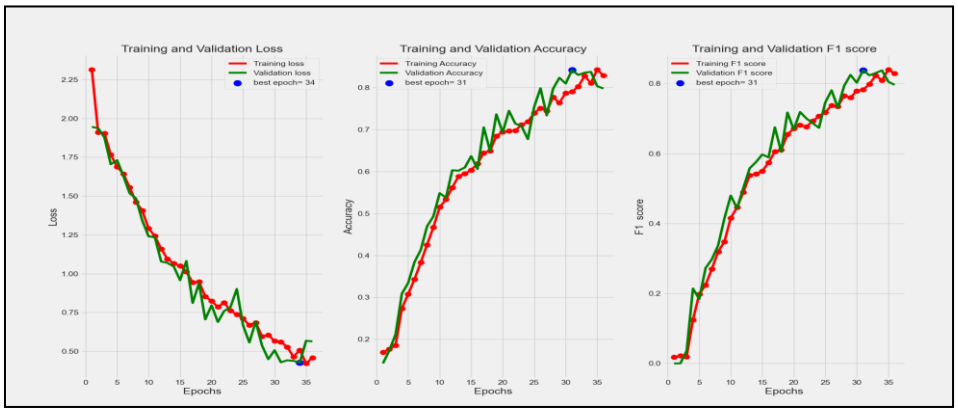

Fig. 5. Training and Validation Curve on epochs for Squeeze Model

V.i. Comparison with Other Methods

A comparative analysis is conducted between our proposed method and existing approaches to better illustrate its effectiveness. Table 5 indicates that our strategy outperformed other networks in terms of performance.

Table 5: Comparison with other Skin Disease Detection and Classification Work

Reference	Dataset Used	Disease	Number of Classes	Model	Accuracy
[XXIV]	ISIC2018	Benign, malignant	2	CNN	83.1%
[XXIII]	ISIC2018	Benign, malignant	2	Resnet50	83.6%
[X]	HAM10000	Actinic keratoses, Benign keratosis, Intraepithelial carcinoma, Dermatofibroma, Basal cell Vascular lesions Melanocytic nevi, Melanoma	7	MobileNet	83.9%
[I]	2-ary, 3-ary, 9-ary	Melanoma, Benign	2	DenseNet	82%
[XX]	ISIC2018	Melanoma, Nevi, and Seborrheic Keratosis	3	VGG19_2	76.6%
Proposed	HAM10000	Basal cell carcinoma , dermatofibroma , Melanoma , Benign Keratosis-like lesions , and Melanocytic nevi	4	Squeeze net	92.93

6. Conclusion

Convolutional neural network design-space exploration has become more methodical due to the several specified steps uncovered in this study. SqueezeNet, a CNN design that uses 50% fewer parameters than AlexNet while maintaining AlexNet-level accuracy on ImageNet, is introduced to accomplish this. SqueezeNet is one of the

new CNNs discovered while thoroughly analyzing the CNN architecture design space. The dataset for skin lesions is taken from HAM10000. The four skin cancer types represented in the dataset are basal cell carcinoma (BCC), benign keratosis-like lesions (BKL), dermatofibroma (DF), melanoma (MEL), and melanocytic nevi (NV). Our SqueezeNet model performed well in identifying skin cancer diseases from the images, with an overall accuracy of 92.25%, precision of 85%, recall of 84%, and F1-score of 83%. On the validation data set, it has been demonstrated that the suggested model has produced amazingly accurate results. For BCC, BKL, DF, MEL, and NV, the trained model achieved accuracies of 93.25%, 90.5%, 93.75%, and 91.75, respectively. Future research will increase the skin disease dataset to include additional types of skin cancer, which will benefit the trained model under difficult circumstances.

Conflict of interest

The authors have no conflicts of interest to declare that are relevant to the content of this article.

References:

I. A. Foahom Gouabou, J. Damoiseaux, J. Monnier, R. Iguernaissi, A. Moudafi, and D. Merad. : 'Ensemble method of convolutional neural networks with directed acyclic graph using dermoscopic images: Melanoma detection application'. *Sensors*, Vo. 21(12), 3999, 2021. 10.3390/s21123999

II. A. Qureshi, and T. Roos. : 'Transfer learning with ensembles of deep neural networks for skin cancer detection in imbalanced data sets'. *Neural Processing Letters*, Vol. 55(4), pp. 4461-4479, 2023. 10.1007/s11063-022-11049-4

III. B. Switzer, I. Puzanov, J. Skitzki, H. Hamad, and M. Ernstoff. : 'Managing metastatic melanoma in 2022: a clinical review'. *JCO Oncology Practice*. Vol. 18(5), pp. 335-351, 2022. 10.1200/OP.21.0068

IV. C. Chang, W. Wang, F. Hsu, R. Chen, H. Chan. : 'AI HAM 10000 Database to Assist Residents in Learning Differential Diagnosis of Skin Cancer'. *IEEE 5th Eurasian Conference on Educational Innovation (ECEI)*. IEEE. pp. 1-3. 2022, February. 10.1109/ECEI53102.2022.9829465

V. C. Kaushal, S. Bhat, D. Koundal, and A. Singla. : 'Recent trends in computer assisted diagnosis (CAD) system for breast cancer diagnosis using histopathological images'. *Irbm* Vol. 40(4), pp. 211-227, 2019. 10.1016/j.irbm.2019.06.001

VI. C. Scard, H. Aubert, M. Wargny, L. Martin, and S. Barbarot. : 'Risk of melanoma in congenital melanocytic nevi of all sizes: A systematic review'. *Journal of the European Academy of Dermatology and Venereology*. Vol. 37(1), pp. 32-39, 2023. 10.1111/jdv.18581.

VII. F. Mallat, S.Matar, and B. Soutou. : 'Umbilical seborrheic keratosis-like lesion developing after diode laser hair removal in an 18-year-old patient'. *Journal of Cosmetic and Laser Therapy*. Vol.25(1-4), pp. 54-56, 2023. 10.1080/14764172.2023.2241690.

VIII. J. Tembhurne, N. Hebbar, H. Patil, and T. Diwan T., : 'Skin cancer detection using ensemble of machine learning and deep learning techniques'. *Multimedia Tools and Applications*. Vol. 82. pp. 27501-27524, 2023. 10.1007/s11042-023-14697-3

IX. L. Steele, X. Tan, L. Olabi, B. Gao, J. Tanaka, and H. Williams. : 'Determining the clinical applicability of machine learning models through assessment of reporting across skin phototypes and rarer skin cancer types: a systematic review'. *Journal of the European Academy of Dermatology and Venereology*. Vol. 37(4), pp. 657-665, 2023. 10.1111/jdv.18814

X. M. Alnowami. : 'Very Deep Convolutional Networks for Skin Lesion Classification'. *J. King Abdulaziz Univ. Eng. Sci*. Vol. 30, pp. 43-54, 2019. 10.4197/Eng. 30-2.5

XI. M. Hu, Y.Li, Y, and X. Yang. : 'Skinsam: Empowering skin cancer segmentation with segment anything model'. *arXiv preprint arXiv:* 2304.13973, 2023. 10.48550/arXiv.2304.13973

XII. M. Llamas-Velasco, T. Mentzel, E. Ovejero-Merino, E. M. Teresa Fernández-Figueras, and H. Kutzner. : 'CD64 staining in dermatofibroma: A sensitive marker raising the question of the cell differentiation lineage of this neoplasm'. *Journal of Molecular Pathology*. Vol. 3(4), pp. 190-195, 2022. 10.3390/jmp3040016

XIII. N. Ceylan, S. Kaçar, E. Güney, and C. Bayilmiş. : 'Detection of Grinding Burn Fault in Bearings by Squeeze Net'. *30th Signal Processing and Communications Applications Conference (SIU).* IEEE. pp. 1-4, 2022, May. 10.1109/SIU55565.2022.9864895

XIV. N. Kumar and T. Sandhan. : 'Alternating Sequential and Residual Networks for Skin Cancer Detection from Biomedical Images'. *National Conference on Communications (NCC).* IEEE. pp. 1-5, 2023, February. 10.1109/NCC56989.2023.10068074

XV. N. Trivedi, V. Gautam, A. Anand, H. Aljahdali, S. Villar, D. Anand, and S. Kadry,: 'Early detection and classification of tomato leaf disease using high-performance deep neural network'. *Sensors*. Vol. 21(23), 7987, 2021. 10.3390/s21237987

XVI. P. Dhiman, A. Kaur, Y. Hamid,E. Alabdulkreem, H. Elmannai, and N. Ababneh. : 'Smart Disease Detection System for Citrus Fruits Using Deep Learning with Edge Computing'. *Sustainability*. Vol. 15(5), 4576, 2023. 10.3390/su15054576

XVII. P. Dhiman, V. Kukreja, and A.Kaur. : 'Citrus fruits classification and evaluation using deep convolution neural networks: an input layer resizing approach'. *2021 9th International Conference on Reliability, Infocom Technologies and Optimization, (Trends and Future Directions) (ICRITO)*. IEEE. pp. 1-4, 2021, September. 10.1109/ICRITO51393.2021.9596357

XVIII. R. Jain, S. Dubey, and G. Singhvi. : 'The Hedgehog pathway and its inhibitors: Emerging therapeutic approaches for basal cell carcinoma'. *Drug discovery today*. Vol. 27(4), pp. 1176-1183, 2022. 10.1016/j.drudis.2021.12.005

XIX. S. Aggarwal,S. Gupta, A. Alhudhaif, D. Koundal, R. Gupta, and K. Polat. : 'Automated COVID-19 detection in chest X-ray images using fine-tuned deep learning architectures'. *Expert Systems*. Vol. 39(3), e12749, 2022. 10.1111/exsy.12749

XX. T. Mazhar, I. Haq, A. Ditta, S. Mohsan, F. Rehman, I. Zafar, and L. Goh, : 'The role of machine learning and deep learning approaches for the detection of skin cancer'. *Healthcare*. MDPI. Vol. 11(3), 415, 2023, February. 10.3390/healthcare11030415

XXI. V. Anand, S. Gupta, A. Altameem, S. Nayak, R. Poonia, and A. Saudagar. : 'An enhanced transfer learning based classification for diagnosis of skin cancer'. *Diagnostics*. Vol. 12(7), 1628, 2022. 10.3390/diagnostics12071628

XXII. V. Anand, S. Gupta, D. Koundal, S. Mahajan, A. Pandit, and A. Zaguia. 'Deep learning based automated diagnosis of skin diseases using dermoscopy'. *Computers, Materials & Continua*. Vol. 71(2), pp. 3145-3160, 2022. 10.32604/cmc.2022.022788

XXIII. W. Gouda, N. Sama, G. Al-Waakid, M. Humayun, and N. Jhanjhi. : 'Detection of skin cancer based on skin lesion images using deep learning'. *Healthcare*. *MDPI*. Vol. 10(7), 1183, 2022, June. DOI:10.3390/healthcare10071183.

XXIV. Y. Dahdouh, A. Anouar Boudhir, and M. Ben Ahmed. : 'A New Approach using Deep Learning and Reinforcement Learning in HealthCare: Skin Cancer Classification'. *International journal of electrical and computer engineering systems*. Vol. 14(5), pp. 557-564, 2023. 10.32985/ijeces.14.5.7